Progress In Electromagnetics Research, PIER 30, 157–178, 2001

ANTENNA MEASUREMENTS IN THE PRESENCE OF MULTIPATH WAVES

H.-J. Li, T.-Y. Liu, and J.-L. Leou

Department of Electical Engineering &
Graduate Institute of Communication Engineering
National Taiwan University
Taipei, Taiwan, R.O.C.

Abstract–In this paper antenna measurements in the presence of multipath waves are discussed. Methods are proposed to diagnose the degradation sources of a compact range measurement system operating at a frequency much lower than the designed frequency range. A range-gating technique is employed to improve the capability of the compact range measurement system. With this technique, the field responses over a bandwidth for each rotation angle are coherently measured, and the fast Fourier transform is applied to obtain the range profile. A suitable window function is applied to extract the desired path and eliminate all other undesired paths. The antenna pattern is plotted according to the filtered response of the desired path. We have expressed the receiving voltage of a testing antenna in terms of its gain pattern and input impedance of the testing antenna operating in multipath environment. If the bandwidth of the testing antenna is very narrow and the mismatch problem is very serious over the required bandwidth, an algorithm is proposed to compensate the mismatch effect so that the obtained radiation pattern and the antenna gain are more accurate. Numerical and experimental results have verified the effectiveness of our method.

1. INTRODUCTION

For antenna pattern or radar cross section (RCS) measurements, the antenna under test or the object should be illuminated by a plane wave. To obtain a plane wave illumination, the separation between the testing antenna or object and the illumination source should satisfy the far-field condition, $2D^2/\lambda$, where D is the dimension of the testing antenna or the object and λ is the operating wavelength. To reduce the separation requirement, compact range systems are usually implemented in an anechoic chamber [1–5]. The quiet zone, defined as the area which is nearly uniformly illuminated, is used to characterize the permissible largest dimension of the testing object.

There are several types of compact range systems. The compact range system in the EM Lab of National Taiwan University is a Two-reflector type and was built by the Chung-Shan Institute of Science and Technology Taipei, Taiwan, ROC. This system is designed for antenna measurements for frequencies higher than $8\,\mathrm{GHz}$. However, our anechoic chamber is not only used for antenna measurements but also used for scattering measurements, and the operating frequency can be below $2\,\mathrm{GHz}$. If the compact range system is not carefully operated its presence in the anechoic chamber will introduce undesirable scattering and degrade the chamber performance. We will show how this compact range system designed for antenna pattern measurements can be used for scattering measurements and how to extend the operating frequency to below $2\,\mathrm{GHz}$.

In this paper we will examine how the measurement performance is degraded when the system is used for scattering measurements and when the operating frequency exceeds its designed range. We will employ microwave imaging technique [6, 7] to diagnose the cause of degradation and propose methods to improve the measurement capability of the compact range system.

In Section 2 the basic properties of a compact range measurement system and practical limitations will be described. The performance of the compact range system when it is used for antenna and scattering measurements will be compared. How the quiet zone is degraded when the operating frequency is beyond the designed range will be demonstrated. The sources causing degradation will be diagnosed. In Section 3 we will discuss antenna measurement techniques in the presence of multipath interference. We will express the received voltage response in terms of the antenna input impedance and radiation pattern. In Section 4 we will propose methods to differentiate different multipaths and propose algorithms to obtain the radiation pattern and antenna gain of a testing antenna. Some numerical and experimental examples will be given in Section 5. Discussion and conclusion will be given in Section 6.

2. DIAGNOSIS OF DEGRADATION SOURCES FOR A COMPACT-RANGE MEASUREMENT SYSTEM

The purpose of a compact-range system is to obtain uniform illumination with a distance much shorter than that required by the far-field condition. There are several different types of compact range measurement systems [1–3]. A sketch of the compact range system at the EM Lab of the National Taiwan University is shown in Fig. 1. A horn feeder is used to illuminate the first reflector. The wave is reflected to the prime reflector and then reflected back to illuminate the testing antenna. This compact-range system is designed to operate at frequencies higher than 8 GHz. To examine the performance of the compact-range system a waveguide-type probe is placed on a linear scanner to measure the magnitude and phase of the received field. Amplitude and phase of the fields received along a straight line are shown by the solid curves in Fig. 2(a) and (b) respectively. It is seen that the phase curve in Fig. 2(b) is almost linearly proportional to the scanner position because the direction of wave arrival is slightly offset to the normal of the scanner. If the linear variation is subtracted from Fig. 2(b), the result is shown in Fig. 2(c). A quiet zone is defined as the region where it is uniformly illuminated. From Fig. 2(a) and 2(c), one can see that the quiet zone is in the center part with a range of about 75 cm. In this region the amplitude variation is smaller than 1 dB and the phase variation is smaller than 5°.

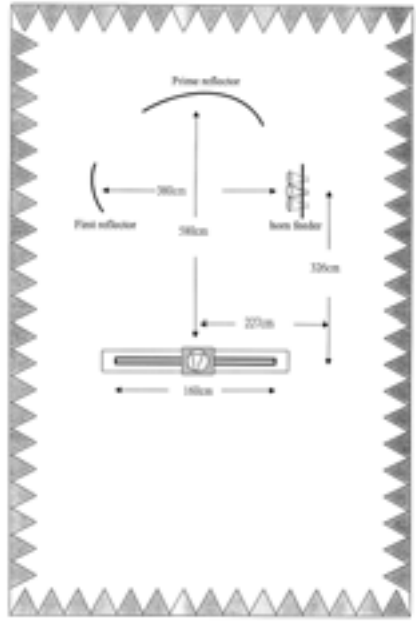

Figure 1. Compact range system at the EM Lab of N.T.U.

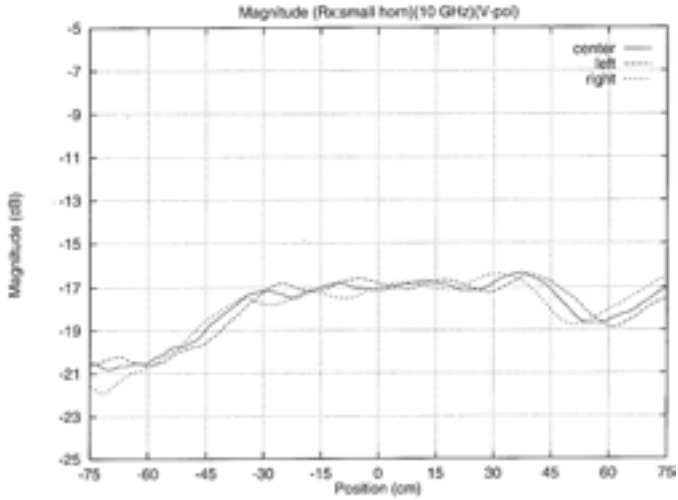

(a)

Figure 2. Amplitude and phase distributions alone a linear scanner for three different feeder positions (a) Amplitude.

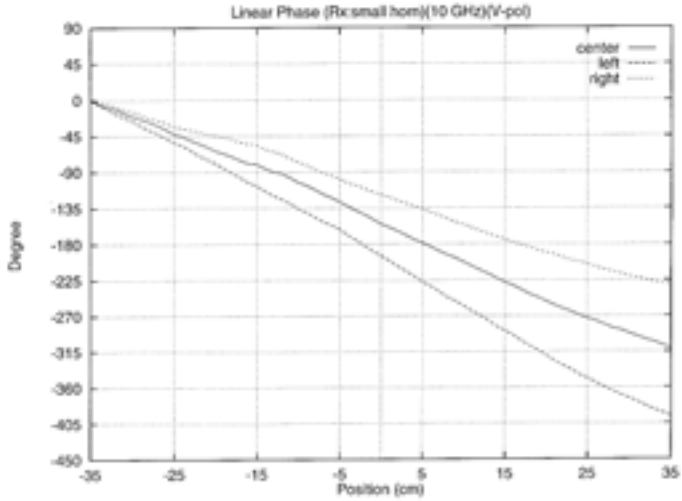

(b)

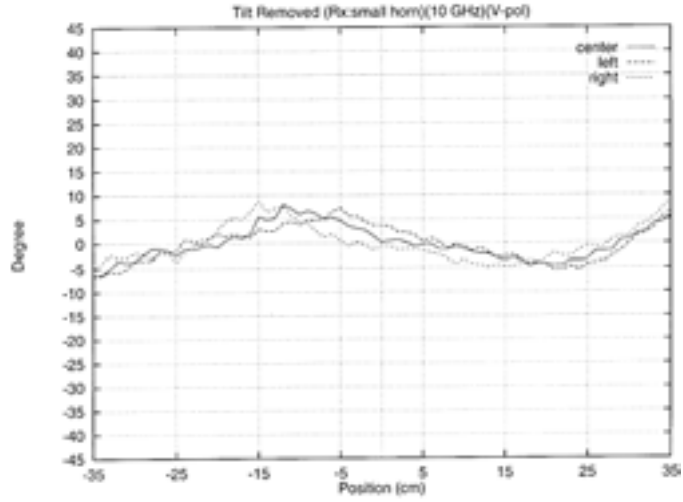

(c)

Figure 2. Amplitude and phase distributions alone a linear scanner for three different feeder positions (b) Phase, (c) Phase when the linear variation of (b) is substrated.

If the compact range system is used for RCS measurement, the testing antenna is replaced by a testing object. To measure the backscattered field, an additional horn antenna should be placed by the side of the illuminating horn. In other words, two antennas are placed side by side, one for transmitting and the other for receiving, and both are offset to the original center position as shown in Fig. 1. With this offset illumination, we again measure the magnitude and phase distribution along the same straight line, and the results are also shown by the dashed curves in Fig. 2. It is seen that with such a small offset in the feeding position, the deviations in the magnitude and phase distribution are small. Therefore we conclude that the compact range system can also be used for scattering measurement.

It is noted that the scanning of a probe along a linear line can be viewed as a synthetic linear array. The direction of the wave arrival can be obtained by taking the Fourier transform of the complex field received along the linear scanner. The derived directions of wave arrivals when the feeding horn is mounted at the center, at the left offset, and at the right offset are respectively shown in Fig. 3. It is seen that the directions of wave arrivals change accordingly.

If we reduce the operating frequency and repeat the field measurement, the amplitude distributions along the line for several different frequencies are shown in Fig. 4. It is seen that the lower the operating frequency is, the larger the amplitude variation is. Notice that the periodic variation in Fig. 4 is the result of interference of multipaths. To see this, we can take the Fourier transform of the field received along the synthetic array for each frequency and obtain the direction of arrival of each path. The results for several different frequencies are shown in Fig. 5. It can be seen that the smaller the frequency, the stronger the multipath components. A strong component comes from the direction of 35°, which is in the direction of the feeding antenna.

In the above we determine the direction of wave arrival by taking the Fourier transform of the fields received along the synthetic array. We can further determine the distances of different paths by measuring the frequency response at a given location and then applying the Fourier transform to the frequency response to obtain the range profile [6, 7]. Fig. 6 shows the range profile obtained at the center frequency 2.5 GHz. The transmitting antenna is a double ridged wideband antenna, and the receiving antenna is a log-periodic antenna pointing

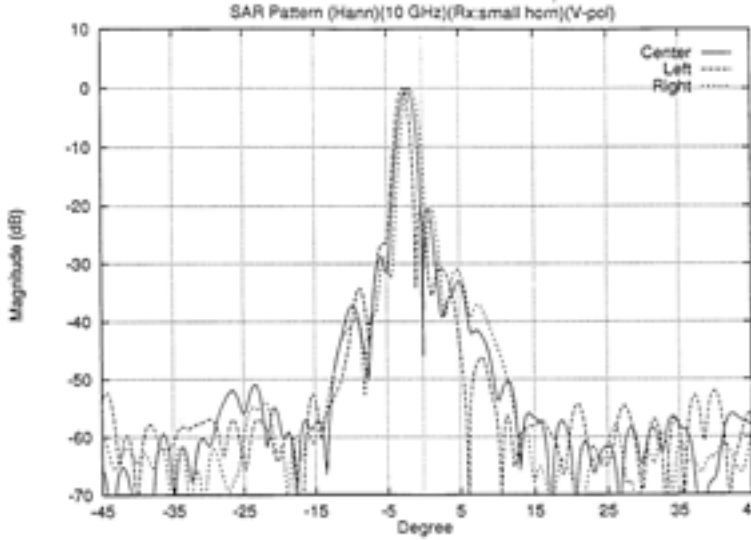

Figure 3. Directions of wave arrivals for three different feeding positions.

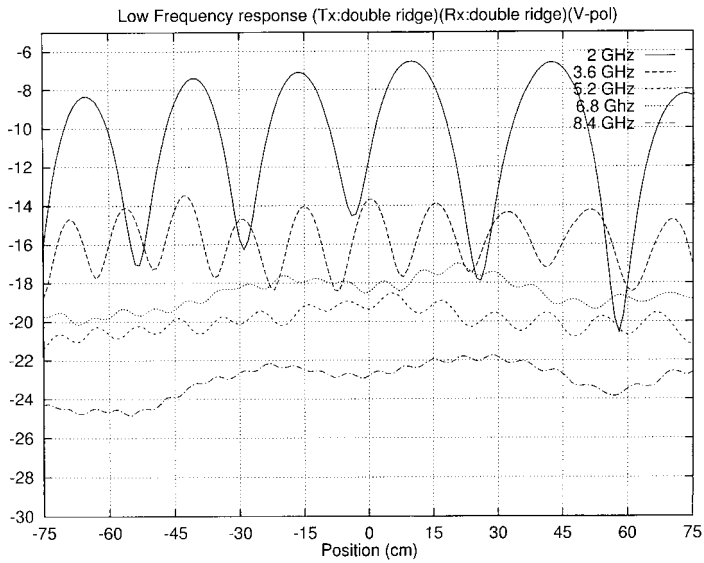

Figure 4. The amplitude distributions for different operating frequencies.

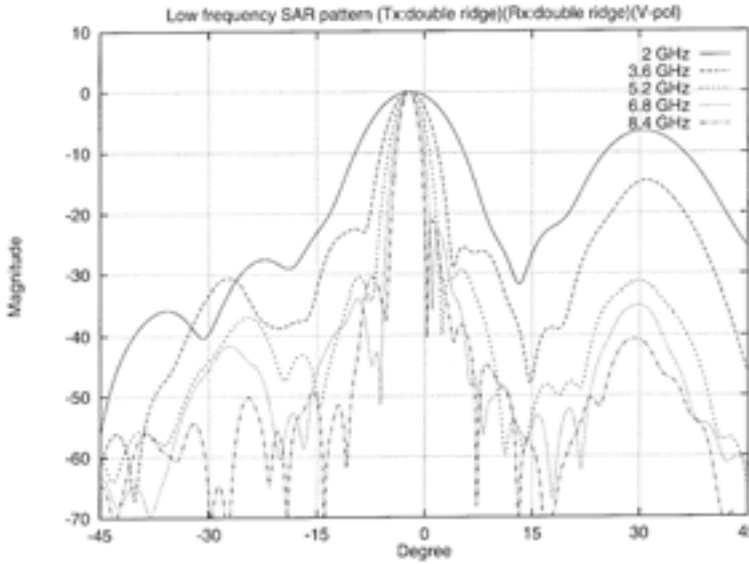

Figure 5. The direction of wave arrival for different frequencies.

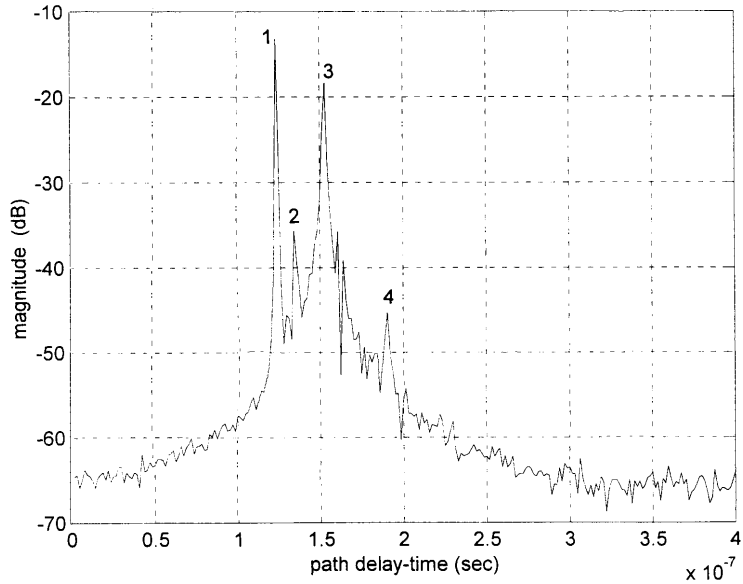

Figure 6. Range profiles with center frequency equal to 2.985 GHz.

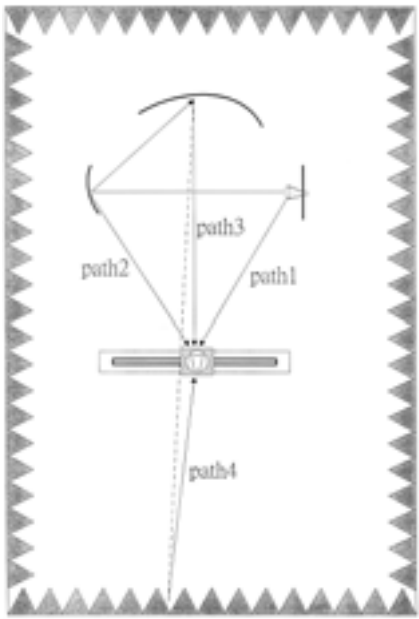

Figure 7. Sketch of multipath of the compact range system for explanation of the range profile of Fig. 6.

to the main reflector. The range profile provides the source of each multipath. These multipaths are sketched in Fig. 7.

3. ANTENNA PATTERN MEASUREMENT IN THE PRESENCE OF MULTIPATHS

In the last section we observed that the presence of multipaths would limit the measurement capability and degrade the performance. In this section we will first express the received voltage in terms of the gain pattern and input impedance of the receiving antenna in the presence of multipaths and then propose a method to differentiate multipaths so that the antenna pattern and the gain can be accurately obtained.

Consider a receiving antenna with input impedance response $Z_{in}(k)$ being connected through a transmission line (with characteristic impedance Z_o and length ℓ) to a receiver with load impedance Z_L. The equivalent circuit is shown in Fig. 8, where $V_{oc}(k)$ is the open circuit of the receiving antenna. Assume $Z_L = Z_o = R_o$, the voltage

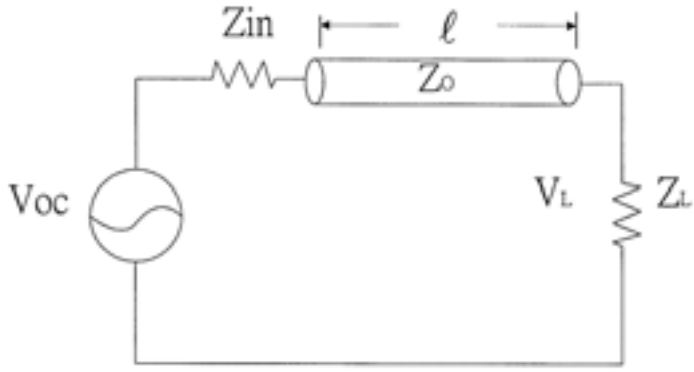

Figure 8. The equivalent circuit of the receiver.

at the receiver $V_L(k)$ can be expressed as

$$V_L(k) = \frac{V_{oc}(k) \cdot R_o \cdot e^{-j2kl}}{Z_{in}(k) + R_o} \tag{1}$$

When the antenna is illuminated by a field incident from direction (θ, ϕ), the open circuit voltage of the receiving antenna can be expressed as [8]

$$V_{oc}(k) = -j\frac{2\pi}{k}\sqrt{\frac{R_{in}(k)G(k,\theta,\Phi)}{\pi\eta}}\hat{e}_t(k,\theta,\Phi) \cdot \vec{E}_1^i(k,\theta,\Phi) \tag{2}$$

where η is the characteristic impedance of free space, $R_{in}(k)$ is the real part of $Z_{in}(k)$, $G(k,\theta,\Phi)$ is the gain pattern of the receiving antenna, $\hat{e}(k,\theta,\Phi)$ is the polarization unit vector of the antenna when it is used as a transmitting antenna, and $\vec{E}_i(k,\theta,\Phi)$ is the incident field at the antenna terminal.

If the antenna is illuminated by multipath waves the open circuit voltage can be expressed as

$$V_{oc}(k) = \sum_m -j\frac{2\pi}{k}\sqrt{\frac{R_{in}(k)G(k,\theta_m,\Phi_m)}{\pi\eta}}\hat{e}_t(k,\theta_m,\Phi_m) \cdot \vec{E}_m^i(k,\theta_m,\Phi_m) \tag{3}$$

where (θ_m, Φ_m) is the arrival direction of the mth component and $\vec{E}_m^i(k,\theta_m,\Phi_m)$ is the mth illuminating field at the terminal.

Let γ_m be the distance of the mth path, and assume that the input impedance, the radiation pattern, and the polarization unit vector are nearly constant over the bandwidth of interest (which is much smaller than the center frequency). Then $V_{oc}(k)$ can be approximated by

$$V_{oc}(k) = V_{oc}(k_o + \Delta k) \cong \sum -j\frac{2\pi}{k_o}\sqrt{\frac{R_{in}(k_o)G(k_o,\theta_m,\Phi_m)}{\pi\eta}}a_m e^{-j\Delta k r_m} \tag{4}$$

where $a_m = \hat{e}_t(k_o,\theta_m,\Phi_m)\cdot\vec{E}^i_m(k_o,\theta_m,\Phi_m)$.

To differentiate the multipath, we can measure $V_L(k)$ over a bandwidth and then apply the Fourier transform to obtain the range profile. The bandwidth should be wide enough so that the desired path can be resolved. With this procedure, the contributions by different paths or the desired paths can be obtained by searching the peak positions and peak values of the range profile.

If the antenna is rotated, the open circuit voltage will be

$$V_{oc}(k,\theta,\Phi) \approx \sum -j\frac{2\pi}{k_o}\sqrt{\frac{R_{in}(k_o)G(k_o,\theta+\theta_m,\theta+\Phi_m)}{\pi\eta}}a_m(\theta,\Phi)e^{-j\Delta k r_m} \tag{5}$$

where $a_m(\theta,\Phi) = \hat{e}_t(k_o,\theta+\theta_m,\Phi+\Phi_m)\cdot\vec{E}^i_m(k_o,\theta+\theta_m,\Phi+\Phi_m)$.

If we measure the frequency response $V_L(k,\theta,\Phi)$ over a bandwidth for each rotation angle and take the Fourier transform, we obtain the range profile. We can identify each path component by searching the corresponding peak of each range profile. Note that amplitude of each peak is proportional to the antenna pattern. By plotting the peak value of a certain path versus the rotation angle we can obtain the radiation pattern.

In the above derivation we have assumed that the radiation pattern and the input impedance are independent of frequency. If the assumption is not valid, then the obtained radiation pattern is the mean pattern averaged over the bandwidth. For example, the null position of a large array or a large aperture antenna is a function of frequency. If the bandwidth used in the above procedure is too large, the null position obtained will not be as deep as that obtained at a single frequency. In that case we can apply following algorithm to obtain the radiation pattern for each certain frequency:

1. Choose a suitable bandwidth so that we can differentiate the desirable path from the other paths.
2. For each rotation angle, measure the frequency response $V_L(k)$ over the bandwidth.
3. Take the Fourier transform of $V_L(k)$ to obtain the range profile at each rotation angle.
4. Multiply the range profile with a suitable window function centered at the peak position of the desired path so that only the desired path can pass through and all other multipaths are attenuated.
5. Take the Inverse Fourier transform of the range profile of the desired path to obtain the filtered voltage response $V'_L(k, \theta, \Phi)$ for each rotation angle.
6. The radiation pattern for certain frequency k can be obtained by plotting $V'_L(k, \theta, \Phi)$ versus rotation angle.

4. ANTENNA GAIN MEASUREMENT IN THE PRESENCE OF MULTIPATHS

The antenna gain of a testing antenna is usually obtained by comparing the voltages received by the testing antenna and by a standard antenna with a known gain value. In the presence of multipaths, the antenna gain can be obtained by the following procedure.

1. Replace the testing antenna by a standard antenna with a known gain value.
2. Measure the frequency response. The bandwidth and the frequency points must be the same as those used in measuring the testing antenna. Apply the inverse Fourier transform on the frequency response to obtain the range profile.
3. Record the peak value of the desired path.
4. The gain of the testing antenna is obtained by taking the ratio of the peak value obtained in the case of testing antenna over the peak value obtained in the case of standard antenna.
5. Or apply the same window function to retain the desired path and eliminate all other paths, and then take the inverse Fourier transform to obtain the filtered frequency response. The gain of the testing antenna at a certain frequency is obtained by comparing the ratio of the two filtered responses at that frequency.

If the testing antenna is a narrowband antenna, there will be a mismatch between the antenna and the receiver over the bandwidth. It is also noted that in Eq. (1) and Eq. (2) the received voltage $V_L(k)$ is a function of the antenna input impedance $Z_{in}(k)$. A mismatch in impedance will reduce the load voltage. If we apply the Fourier transform to the frequency response $V_L(k)$ to obtain the range profile, the range resolution will become poorer and the peak value will decrease. If the bandwidth is too narrow, it may not be able to resolve the desired path and the derived antenna gain value can be inaccurate.

The reflection coefficient $|\Gamma(k)|$ of a testing antenna usually can be measured. It is known that the power delivered to the receiver will be reduced by a factor of $1-|\Gamma(k)|^2$ due to a mismatched impedance [3]. If we correct the measured $V_L(k)$ with a factor of $1/\left[1-|\Gamma(k)|^2\right]^{1/2}$ and then follow the procedure described in the previous section, we can obtain a more accurate measurement of the range profile and the antenna pattern and the gam value.

5. NUMERICAL AND EXPERIMENTAL RESULTS

In this section we will show some numerical and experimental examples to demonstrate the effectiveness of the proposed method.

In our anechoic chamber we mount a directional antenna on a pedestal which can be rotated, and measure the frequency response over a frequency bandwidth for each rotation angle. We then apply the Fourier transform to each frequency response and use the window method to isolate each path component, and then plot the receiving pattern of each path component. From the pattern plots we can obtain the amplitude, the time delay, and the arrival direction of each path component for the imperfect compact range measurement system. The parameters obtained for center frequency 2.985 GHz are shown in Table 1.

5.1 Example 1

These parameters are then being used for the following simulations. Assume that the testing antenna is a linear broadside antenna array with spacing d and a total of $N+1$ elements. The array factor can be expressed as

$$AF(k,\phi)=\frac{\sin(kNd\cos\phi)}{kd\cos\phi} \tag{6}$$

Table. 1 Path parameters of $Fc = 2.985\,\text{Ghz}$.

Paths	Time-Delay (nsec)	Amplitude	Arrival-Angle (deg.)
1	122	1	40
2	133	0.092	-20
3	151	0.92	0
4	187	0.0366	190

Assume that the input impedance of the antenna array is matched to that of the receiver over the frequency bandwidth. The field received at frequency k and rotation angle ϕ can be expressed as [9]

$$E(k,\phi) = \sum_{i=1}^{4} a_i \frac{\sin[kNd\cos(\phi-\phi_i)]}{kd\cos(\phi-\phi_i)} \tag{7}$$

The theoretical value of $AF(k,\phi)$ versus ϕ for $f = 2.985\,\text{GHz}$, $d = 5\,\text{cm}$ and $N = 21$ is shown in Fig. 9(a). The plot of $E(k,\phi)$ versus ϕ for $f = 2.985\,\text{GHz}$ is shown if Fig. 9(b). It is seen that the existence of multipath distorts the radiation pattern. For each rotation angle we calculate the frequency response over a bandwidth of $500\,\text{MHz}$, apply the inverse Fourier transform to obtain the range profile, and find the peak value of the desired path. We plot the peak value versus rotation angle and the resultant antenna pattern is shown in Fig. 9(c). It is seen that the nulls of Fig. 9(c) are not as deep as those in Fig. 9(a) due to the averaging effect. We conclude that a bandwidth of $500\,\text{MHz}$ ($1/6$ of the center frequency) is too broad for obtaining such an array pattern. If we reduce the bandwidth to $100\,\text{MHz}$ (it is wide enough to resolve all path components in the example), the result is shown in Fig. 9(b). It is seen that the pattern of Fig. 9(b) is much closer to that of Fig. 9(a).

5.2 Example 2

Next we demonstrate the effect of impedance mismatch on the antenna measurements. Fig. 10(a) shows the return loss of a real microstrip antenna element. The corresponding input impedance responses (real part and imaginary part) are shown in Fig. 10(b). We assume that the antenna array of the previous example has the same input impedance response as that of Fig. 10(b), where the bandwidth

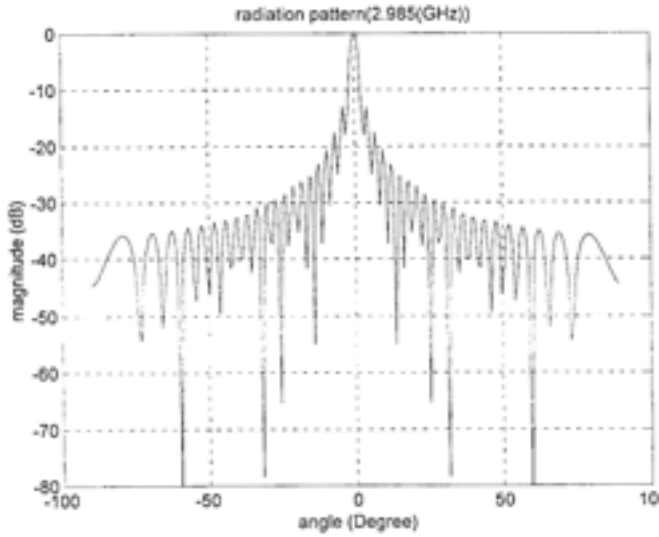

(a)

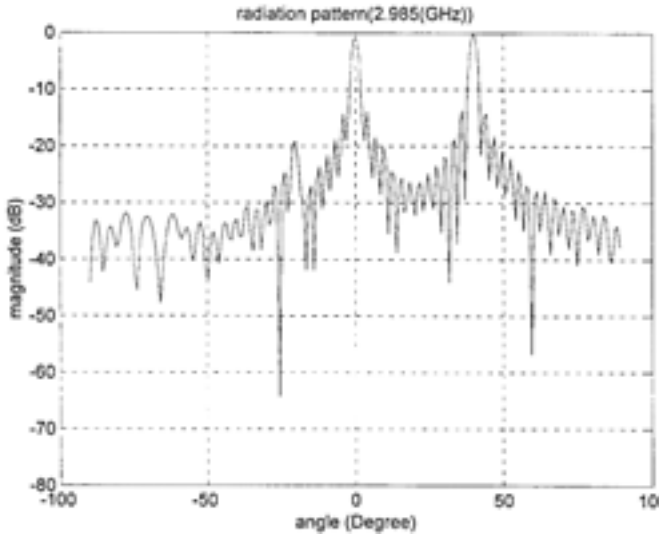

(b)

Figure 9. Antenna patterns of a linear array (a) Theoretical pattern, (b) Pattern obtained in the presence of multipath.

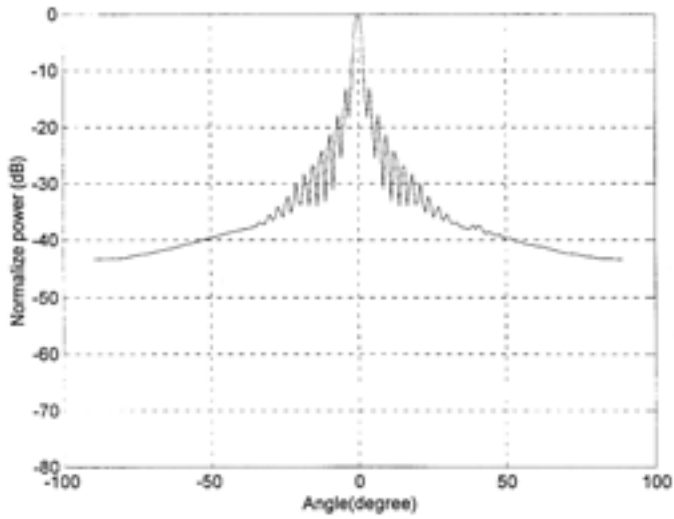

(c)

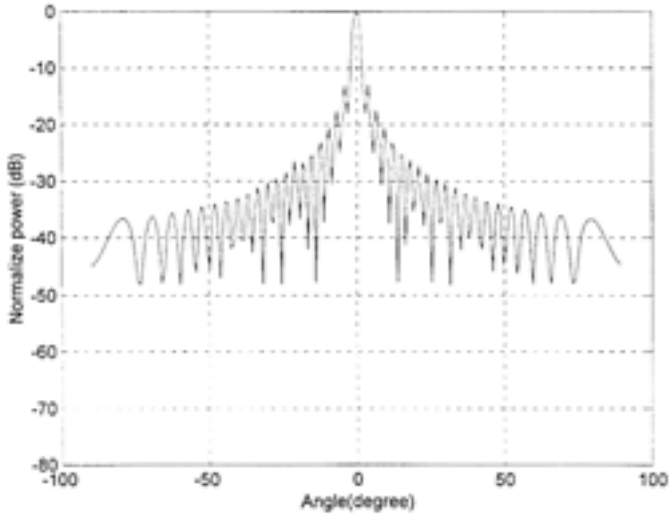

(d)

Figure 9. Antenna patterns of a linear array (c) Pattern obtained after range gating with B.W. = 500 MHz, (d) Pattern obtained after gating with B.W. = 100 MHz.

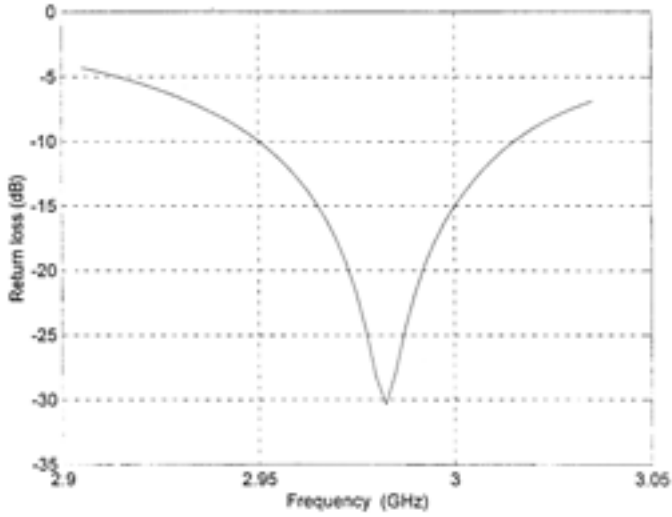

(a)

Figure 10a. The return loss of a microstrip antenna element.

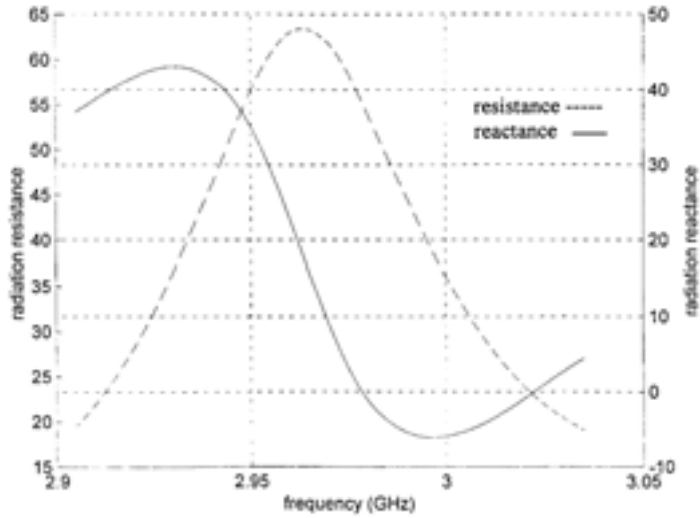

(b)

Figure 10b. The input impedance (real part and imaginary part) of a microstrip antenna element.

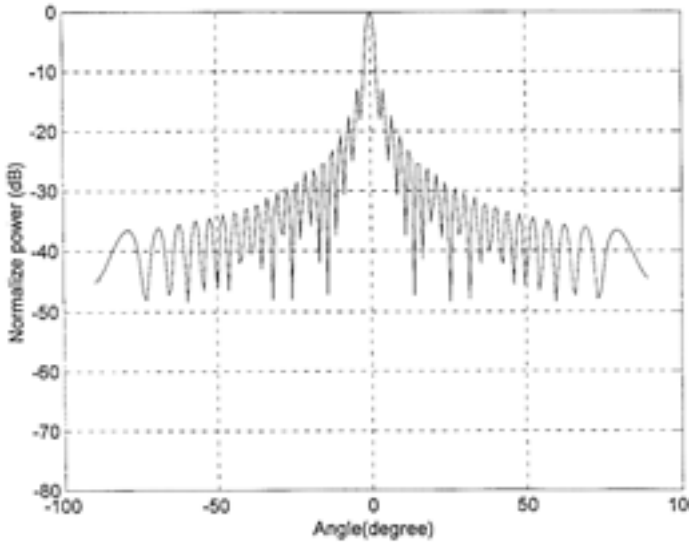

Figure 11. Pattern obtained after range gating with input impedance of Fig. 10.

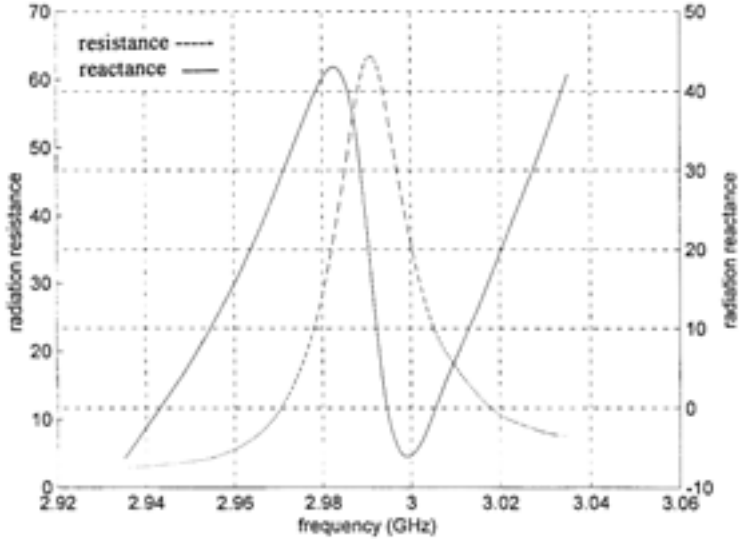

Figure 12. Input impedance with narrowed down bandwidth of Fig. 10.

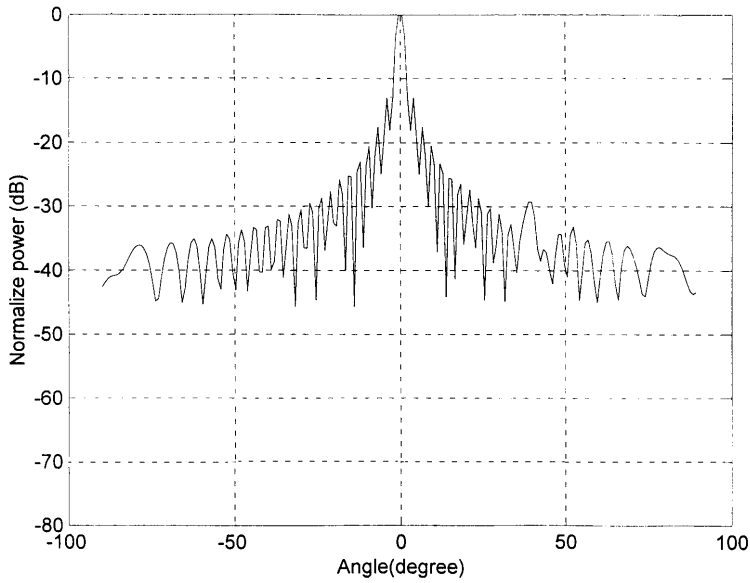

Figure 13. Pattern obtained after range gating with input impedance of Fig. 12.

(defined as the region with return loss $\geq$ 10 dB) is about 60 MHz. We then calculate the frequency response $V_L(k)$ over a bandwidth of 100 MHz, and apply the window algorithm to find the radiation pattern and the gain value. The resultant pattern is shown in Fig. 11. The ratio of the two maximum values of Fig. 9(b) and Fig. 11, corresponding to the impedance matching and mismatching cases respectively, is 0.9724. It is seen that an impedance response like Fig. 10(b) doesn't affect the measurement performance.

If we artificially reduce the bandwidth to 1/4 of the original value and assume that the impedance response is as shown in Fig. 12, then repeating the same procedure we obtain the radiation pattern shown in Fig. 13 and the ratio of the two maximum values of Fig. 9(b) and Fig. 13 becomes 0.6833. It is seen the gain value decreases by a factor of 3.3 dB due to averaging effect of the mismatch loss. If we compensate the voltage response $V_L(f)$ by multiplying a factor of $1/\left[1-|\Gamma(k)|^2\right]^{1/2}$ for each sampled frequency point, the resultant ratio becomes 0.937, which is closer to the ideal value of 1.

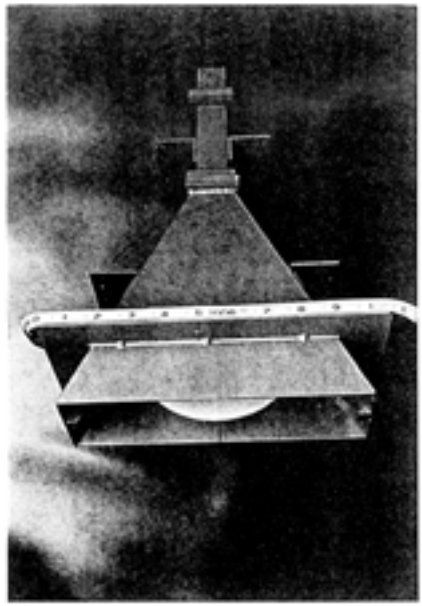

(a)

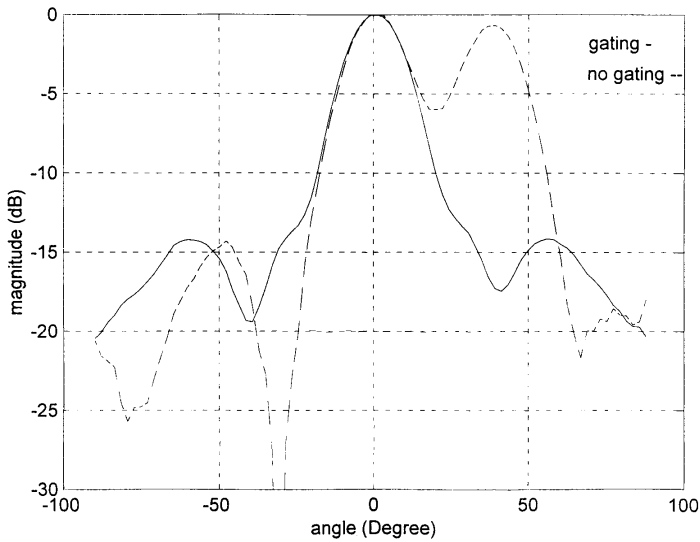

(b)

Figure 14. (a) Photo of a single-ridge horn. (b) The E-plane radiation patterns of (a) obtained without and with range gating at 2.5 GHz .

5.3 Example 3

Finally we demonstrate an experimental example. Fig. 14(a) shows a ridge horn antenna manufactured by the Chung-Shan Institute of Science and Technology. The measured patterns obtained without and with range gating for the E-plane with center frequency equal to 2.5 GHz are shown in Fig. 14(b). It is seen that after windowing, the multipath effect has been eliminated.

6. DISCUSSION AND CONCLUSION

In this paper we have studied antenna measurements in the presence of multipath waves. We propose methods to diagnose the degradation sources of our compact range measurement system when it is operated in frequency much lower than the designed frequency range. We then propose a window technique to improve the measurement capability and show that the operating frequency of the compact range system can be extended to below 2 GHz without having to change the feeder horn and satisfactory performance can still be obtained.

With this technique, the field responses over a bandwidth for each rotation angle are coherently measured, and the fast Fourier transform is applied to obtain the range profile. A suitable window function is then applied to extract the desired path and eliminate all other paths. The antenna pattern is finally plotted according to the filtered response of the desired path. It is noted that the required bandwidth depends on the separation between the desired path and its closest adjacent path. We have expressed the receiving voltage in terms of the gain pattern and input impedance of the testing antenna. However, if the bandwidth of the testing antenna is very narrow and the mismatch problem is very serious over the required bandwidth, then the radiation pattern and the antenna gain obtained can be inaccurate. We have proposed a compensation algorithm so that this mismatch effect can be reduced and the radiation pattern and the antenna gain can be more accurately obtained. Numerical and experimental results have verified the effectiveness of our method.

REFERENCES

1. Evans, G. E., *Antenna Measurement Techniques,* Artech House, Inc., 1990.
2. Hollis, J. S., T. J. Lyon, and L. Clayton, Jr., eds., *Microwave Antenna Measurements,* Scientific Atlanta, Atlanta, 1970.
3. LO, Y. T., and S. W. Lee, *Antenna Handbook,* Van Nostrand Reinhold Company, New York, 1988.
4. Johnson, R. C., ed., "Compact ranges," *Joint Report of TMAT and IEEE A.P.S.,* Philadelphia, June 1986.
5. Burnside, W. D., "Dual chamber design reduces quiet zone ripple/taper errors," *Microwave and RF,* 168–174, May 1987.
6. Li, H. J., N. H. Farhat, Y. Shen, and C. L. Werner, "Image understanding and interpretation in microwave diversity imaging," *IEEE Trans. Antennas Propagate,* Vol. AP-37, No. 8, 1048–1057, 1989.
7. Li, H. J., N. H. Farhat, and Y. Shen, "Image interpretation and prediction in microwave diversity imaging," *IEEE Trans. on Geoscience and Remote Sensing,* 27, 98–101, 1989.
8. Kiang, Y. W., "Antenna receiving characteristics," Private note, Department of Electrical Engineering, National Taiwan University.
9. Elliott, R. S., "Antenna theory and design," Prentice-Hall, Inc., 1981.